

Changes in the surface electronic structure upon martensitic transformation in TiNi and TiPd

S.E. Kulkova,¹ V.E. Egorushkin,² and J.S. Kim, G. Lee and Y.M. Koo³

*¹Institute of Strength Physics and Materials Science of
the Russian Academy of Sciences, 634021, Tomsk, Russia*

²Tomsk State University, 634050, Tomsk, Russia

*³Department of Physics, Pohang University of Science and Technology,
Pohang 790-784, Republic of Korea*

(Dated: November 30, 2018)

Abstract

The electronic structure of some low index surfaces for martensitic $B19'$ -TiNi and $B19$ -TiPd were investigated using the full-potential linearized augmented plane wave method. The alteration of the electronic structure upon martensitic transformation on the surface were analyzed. According to the surface calculations only insignificant changes in the electronic structure near the Fermi level were found as for bulk ground state. The formation of oxides top layers is also discussed. It is shown that the influence of TiNi substrate is insignificant when three oxides layers are formed.

PACS numbers: 71.20.Be, 73.20.At

The electronic structure (ES) of the intermetallic TiNi and TiPd alloys were on the focus of a number of works^{1,2,3,4,5}, due to their unique mechanical properties and technological importance for engineering and medicine. The unusual mechanical properties such as shape memory effect (SME) are connected with martensitic transformations (MT's), which involve the displacements of atoms within the lattice together with the changes of its shape. This is a type of diffusionless structural phase transformation. The MT critical temperature for TiPd is around 840 K that much higher than that for TiNi (~ 333 K). On cooling *B2*-TiNi transforms martensitically to monoclinic *B19'* structure whereas TiPd goes to the orthorhombic *B19* phase. The martensitic transformation sequence in TiNi strongly depends on the composition of the alloy, the doping with other metals, and prior thermochemical history. The results obtained in Refs. 1,2,3,4,5 and the references therein provide an insight into the mechanisms of the phase stability in Ti-based alloys. However, the surface ES of Ti-based alloys is less investigated^{6,7,8} in comparison with the bulk ground state. Many surface phenomena are directly related to the surface electronic structure. To the best of our knowledge, fundamental informations about the surface ES of *B2*-TiPd or martensitic phases of both alloys have not been reported. Since TiNi has found widespread application in medicine in last decade, the investigation of its interactions with different adsorbates, protein or bone tissue is very important task. In order to explain complex processes on the surface at the microscopic level we need to understand the electronic structure of clean Ti-based alloys surfaces first of all. In our previous paper⁷ we have performed as a preliminary step before these calculations, a comparative study of the surface ES in a series of *B2*-Ti*Me* alloys (*Me*=Ni, Co, Fe). We have found the increase of density of states (DOS) at the Fermi level $N(E_F)$ in the surface layers for all Ti-terminated *B2*-Ti*Me* (001) films and also in *B2*-TiNi and TiFe (110) surface layers. The obtained results indicate that the Ti-atoms at the surface possess a high chemical reactivity. Since the surface Fe states are dominant at the Fermi level for both surfaces it is possible to conclude that Fe states are also highly reactive. However, it is necessary to take into account the magnetic ordering for the Fe-terminated (001) surface. The authors of Ref. 9 inferred that the structural instability of the bulk Ti-based alloys is due to the larger Ti states contribution in $N(E_F)$ in comparison with that of *Me*. Our results⁷ showed substantial ES changes in the surface layer for both low index surfaces. These ES changes can alter MT's with respect to the martensitic transformation temperature as well as MT sequence on the surface. Thus MT's on the surface can be

different from those in the bulk. In this paper we present the comparative study of surface ES for TiNi and TiPd martensitic phases.

Using the all-electron first principles technique (the Wien 97 implementation of the full-potential linearized augmented plane wave (FLAPW) method¹⁰ within local density approximation (LDA) for the exchange-correlation potential) we have investigated the surface ES of *B19'*-TiNi and *B19*-TiPd. The surface was simulated by repeated slabs separated by a vacuum region in one direction. The thickness of vacuum was chosen to be equal to the two lattice parameters of the bulk material. A five and seven atomic layer slabs were used for *B2*-TiNi and TiPd (110) and (001) surfaces simulation, whereas for *B19'*-TiNi and *B19*-TiPd surfaces a single slab, which consist of eight atomic layers, were used. The lateral lattice parameters were set to the experimental ones^{11,12} for bulk alloys. Only the ideal martensitic structures were investigated but we estimated the relaxation effects for *B2*-TiNi and *B2*-TiPd (110). The interlayer distances in this case were optimized with Newton dynamics. The core states were treated in a non-relativistic fashion. The *3s*-, *3p*- states for TiNi and *4s*-, *4d*-states for TiPd were treated as the valence band states. The multipole expansion of the crystal potential and electron density inside “muffin-tin” spheres was cut at $l_{max}=10$. Non-spherical contributions to charge density and potential within spheres were considered up to $l_{max}=4$. In the interstitial region the charge density and crystal potential was expanded as a Fourier series with wave vectors up to $G_{max}=10$ a.u.⁻¹. The plane wave cutoff was 4 a.u.⁻¹. The density of states was calculated with 28-36 **k**-points grid in the irreducible part of two-dimensional Brillouin zone (2D BZ) depending on the considered surface. The calculated DOS was smoothed out by a Gaussian function with a width of 0.1 eV to suppress noise. Self-consistency was considered to have been achieved when the total energy variation from iteration to iteration did not exceed 10^{-4} Ry.

The low-temperature martensitic *B19'*-TiNi phase is formed from unit cell twice as large as that of the parent *B2*-phase with corresponding rotation of new cell around *B2* [001] axis and also its shift along *B2* [001] and [110] directions. The martensitic unit cell is compressed along *B2* [001] and [110] directions but it is expanded along $[1\bar{1}0]$. Finally, both Ti and Ni atoms are shifted in the (110) plane, which is monoclinically distorted. Both Ti and Pd atoms are shifted in *B2* [110] and $[1\bar{1}0]$ directions but without monoclinic distortion. The atomic structure of *B19'*-TiNi (100), (010) and (001) surfaces are given in Fig. 1. The *B19'*-TiNi (001) surface has an oblique lattice with the same composition as the parent *B2*

(110) surface. The $B19$ and $B19'$ (010) surface is rumpled with the Ni (Pd) atoms shifted by ~ 0.5 (0.68) Å with respect to Ti positions. Both $B19'$ -TiNi (001) and (010) surfaces are derived from $B2$ -TiNi (110) plane upon MT. The $B19'$ (100) surface is derived from $B2$ (001) plane. In the last case the additional splitting within Ni and Ti layers is occurred (Fig. 1a). This leads to different variants in the surface termination. The splitting of the layers is consequence of the monoclinic distortion of the plane. The corresponding $B19$ -TiPd (100) surface does not have such peculiarity. The ES result for the surface termination with two Ti top layers is given in Fig. 2a. Among three surface considered for martensitic $B19'$ -TiNi, the (010) plane is less distorted in comparison with $B2$ (110) parent plane. It is the coherent boundary between both austenitic and martensitic phases.

Differences in the surface electronic structure of both TiNi and TiPd alloys are reflected on the densities of states in Fig. 2, where the Fermi level is set to zero. For both austenitic and martensitic phases, the local DOS (LDOS) at the central layers display similar features to those of the bulk. We found that bulk region is correctly reproduced in all surface ES calculations. As seen from Fig. 3 the LDOS curves obtained in bulk calculation for $B19'$ -TiNi coincide well with those for central layers in surface calculations. This fact reveals that the perturbation of vacuum is well screened within the first few atomic layers from the surface. We can conclude that upon MT surface ES changes in the same way as in bulk alloys³ (a small decrease of $N(E_F)$ in martensitic phase in comparison with austenitic one). Basically the redistribution of the states near E_F is observed. The d -bands of the alloys components become narrower in the surface layer. The change of ES is less for $B19'$ -TiNi (001) surface despite the fact that it is most distorted plane. It was derived from the $B2$ (110) by following distortion: the change of the angle between two axes and the corresponding compression in one direction but the expansion in other one. In addition the Ti and Ni atoms are shifted in the plane with respect to their positions in the parent $B2$ -phase. The Fermi level is dominated by Ti-states as in $B2$ (110). Moreover, it lies exactly in a small DOS peak that may be the indication of the instability of this surface. The same feature is found for $B19$ -TiPd (001) surface but in this case the DOS peak is more broadened.

One the possible mechanism of surface reconstruction is the displacement of Ni (Pd) atoms with respect to Ti atoms that leads to rumpled surface structure. As seen from Fig. 1b the idealized $B19'$ - and $B19$ (010) structures are rumpled ones. This plane is genetically derived from $B2$ ($1\bar{1}0$) with slight compression in both directions upon MT. Initially in the

$B2$ ($1\bar{1}0$) plane the Ti atoms are already shifted with respect to Ni or Pd atoms during surface relaxation as follows from our calculations. Both Ti and Ni(Pd) atoms display a general downward movement. The obtained values of relaxation are -6.7% , -1.96% for Ti and Pd respectively in $B2$ -TiPd (110) and -6.1% , -15.2% for Ti and Ni atoms in $B2$ -TiNi (110). The striking feature of a sharp decrease of $N(E_F)$ is found in the surface layer for $B19'$ -TiNi (010). The Fermi level lies in the local minimum of DOS similarly to the bulk.^{3,5} The shape of Ni LDOS changes substantially whereas the occupancies of the Ni-bonding orbitals are practically the same as for $B19'$ -TiNi (001) surface. Moreover, the $B19'$ -TiNi (010) surface has the lower total energy value in comparison with other cases. We infer that the $B19'$ -TiNi (010) surface is the free energy surface and the growth of the crystal will be preferable in this plane. This is in good agreement with the experimental results.¹³ We would like to emphasize that the displacements of atoms during relaxation in initial $B2$ -TiNi (110) system are partially the same, which is realized upon MT. Thus the $B2$ -TiNi (110) surface is most preferable for martensitic reconstruction. It is believed that the $B2$ -TiNi (110) surface relaxation can stimulate MT. So the parent $B2$ -TiMe (110) surface, where Me is $3d$ - $5d$ transition elements is partially prepared due to relaxation mechanism to future martensitic transformations. Nevertheless this feature cannot be the only driving force of the phase transformation. For example $B2$ -TiFe (110) has the same ruffled surface structure but TiFe does not undergo MT. It is well known that TiFe has a very stable $B2$ -phase in the TiFe-TiCo-TiNi-TiPd series. The ES peculiarities of the parent phase are very important in this context and the local effects can affect considerably MT with respect to martensitic temperature as well as martensite structure. A small amount of Fe (~ 1 - 2%) leads to essential decrease of MT.⁹ The addition of Cu or Pd in $B2$ -TiNi matrix leads to $B2$ - $B19$ MT. The role of the interface will be investigated in more details in our forthcoming paper. Our results indicate that processes in the $B2$ (110) can be fundamental. At the present time it will be interesting to understand the influence of the alloying on the relaxation phenomena and to link them with the corresponding change of the MT temperature. The attempts to find the correlation between the changes in the MT temperature and bulk ES were recently made.^{9,14} It is evident that if the $B2$ (110) surface can be prepared due to relaxation mechanism to future MT, it might lead to a decrease of the energy needed for this transformation.

In the case of $B19'$ -TiNi (100) surface the presence of Ti-surface states near the Fermi

level indicates the high chemical reactivity of this surface as well as parent $B2\text{-TiNi}$ (001). The $B19\text{-TiPd}$ (100) structure has a sharp peak at E_F but the Fermi level is slightly shifted from it for $B19'$ structure due to additional splitting within Ni and Ti layers, which does not occur in the $B19\text{-TiPd}$ (100) system. So, the splitting of layers can stabilize this structure at the surface. In both cases Ti atoms are highly reactivity on the surface. We simulate the decrease of the Ti concentration (additional calculation without one Ti surface layer was performed) but this effect does not lead to substantial DOS change near E_F . We analyzed also the DOS differences between surface and central layers in both austenitic and martensitic phase for all considered surfaces. The lowering of symmetry in martensitic phase leads to splitting of the surface states and their displacement along the energy scale. In general, the similar changes at the surfaces are observed in both alloys. The detailed analysis showed that the number of states and their orbital composition changes insignificantly upon MT. The alteration of the surface ES in TiPd upon MT is found be similar to TiNi. However, the DOS results for both $B19\text{-TiPd}$ (010) and (100) surfaces indicate their instability. It seems that the monoclinic distortion is a consequence of the instability of the $B19\text{-TiNi}$ (010) surface, as in the bulk.³ Actually the appearance of the monoclinic phase is due to the coexistence of the R-type¹⁵ and orthorhombic distortion.

Thus, we can conclude that the mechanisms promoting the MT in the bulk can similarly give rise to that at the surface. In the bulk the atomic bonding can be changed with deviation from stoichiometry, defects, etc. However, even uniform change in the interface region due to impurity can lead to non-uniform displacements of the atoms along the direction, which is perpendicular to the considered plane. This can develop the mechanism, which was discussed above for the surface. The investigation of the influence of impurities on the interface behavior is in progress now.

It is assumed that a biocompatibility of TiNi is related to the presence of titanium oxides on the surface. Since TiNi-based alloys are used for bone, teeth implants and others medical applications, it is desirable to understand the different kind of the interactions on the metal oxide surface in that number with human tissue. The formation of the surface oxide layer could be also considered on $B2\text{-TiNi}$ (110) surface. We simulated the TiO_2 (100) formation on the $B2\text{-TiNi}$ (110) surface. Our slab consists of three layers of TiNi and four, six layers of oxide. It is evident that we used a very simplified model. The situation in the interface region can be very complicated and depends very much on the O coverage. The oxygen

incorporation can induce a substantial distortion of the alloy lattice. In our case the lattice parameters differ slightly as they are 4.594 Å and 2.98 Å for TiO₂ (100) and 4.264 Å and 3.015 Å for TiNi(110). The layer resolved DOS curves for TiO₂ on the TiNi substrate are given in Fig. 4a. We investigated also TiO₂ (100), (001) and (110) surfaces and found that our results are in consistent with previous ones reported in Refs. 16,17,18 and references therein. Since TiO₂ surfaces have been the subject of numerous works we will not describe the result here. It should be noted that basically the results were discussed in the earlier papers with respect to band gap states, which have been observed in the photoemission experiments as well as on oxygen deficient TiO₂(100) and (110) surfaces and also the surface reconstruction. It was shown that oxygen vacancies play a crucial role in the formation of the defects phases, the surface reconstructions and electronic properties of oxides layers. We did not found band gap states for stoichiometry composition in all considered surfaces. The obtained DOS's for clean TiO₂ (100) surface are presented in Fig. 4b. As seen from Fig. 4 the influence of TiNi substrate is insignificant when three oxides layers are formed. The same result was obtained even for the two oxides layers. Since our DOS curves were smoothed, there is effect of the presence of the states in band gap. Thus the obtained results allow us to confirm the assumption made in Ref. 17 that the properties of TiO₂ layers will be important in order to describe the interactions of TiNi implants with different tissue from first principles.

To summarize, we have investigated the surface electronic structure and its change upon MT for two SME alloys using FLAPW method. The obtained results allow us to draw the conclusion that the *B2* TiNi (110) surface is most preferable for martensitic reconstruction and surface relaxation can stimulate the martensitic transformations. Nevertheless only surface cannot be the only driving force for MT but the surface phenomena can influence MT with respect to martensitic temperature. The coherent boundary between austenite-martensite may be also the surface free energy. This fact together with observed ES changes in the *B19'* (010) surface allow us to conclude that growth of TiNi crystal will be preferable in this plane. MT does not influence considerable the surface states and their interaction with different adsorbates also, it is believed. The obtained ES of investigated surfaces in both austenitic and martensitic TiNi and TiPd phases showed that Ti atoms are highly reactive. This explains the existence of titanium oxides film at the TiNi surface. The simulation of oxides film growth on the TiNi (110) substrate was performed.

ACKNOWLEDGMENTS

This work was jointly supported by the Russian Foundation for Basic Research (grant N 02-02-16336), by the Korea Science and Engineering Foundation (KOSEF-2002) and by POSTECH basic research fund.

-
- ¹ D. A. Papaconstantopoulos and D. J. Nagel, *Int. J of Quantum Chem.* **5**, 515 (1971).
 - ² G. L. Zhao *et al.*, *Phys. Rev. B* **40**, 7999 (1989).
 - ³ S. E. Kulkova, V. E. Egorushkin, and V. V. Kalchkhin, *Solid State Commun.* **77**, 667 (1991); S. E. Kulkova, D.V. Valujsky, and I. Yu. Smolin, *Fiz. Tverd. Tela (St. Petersburg)* **43**, 706 (2001).
 - ⁴ G. Bihlmayer, R. Eibler, and A. Neckel. *Ber Bunsenges. Phys. Chem.* **96**, 1625 (1992); *J. Phys.:Condens. Matter.* **5**, 5083 (1993).
 - ⁵ M. Sanati, R. C. Albers, and F. J. Pinski, *Phys. Rev. B* **58**, 13 590 (1998).
 - ⁶ G. Canto, R. De Coss, and D. A. Papaconstantopoulos, *Surf. Rev. Lett.* **6**, 719 (1999); G. Canto, and R. De Coss, *Surf. Sci.* **465**, 59 (2000).
 - ⁷ G. Lee, J. S. Kim, Y. M. Koo, and S.E. Kulkova, *Phys. Low-Dim. Struct.*, **5/6**, 19 (2001); *ibid.*,**11/12**, 89 (2001); S. E. Kulkova, D. V. Valujsky, G. Lee, J. S. Kim, and Y.M. Koo, *Phys. Rev. B* **65**, 12 541 (2002); Lee, J. S. Kim, Y. M. Koo, and S.E. Kulkova, *Int. J. Hydrogen Energy* **27**, 403 (2002).
 - ⁸ Yu. M. Koroteev, A. G. Lipnitskii, E. V. Chulkov, and V. M. Silkin, *Surf. Sci.* **507-510**, 199 (2001).
 - ⁹ S. A. Shabalovskaya, *Phys. Stat. Sol. (b).* **132**, 327 (1985); S. Shabolovskaya, A. Narmonev, O. Ivanova, A. Dementjev, *Phys. Rev. B* **48**, 13 296 (1993).
 - ¹⁰ P. Blaha, K. Schwarz, and J. Luitz, *WIEN97*, (Karlheinz Schwarz, Techn. Univ., Vienna, 1999) [improved and updated Unix version of the origin copyrighted WIEN-code of P. Blaha, K. Schwarz, P. Sorantin, and S. B. Trickey, *Comput. Phys. Commun.* **59**, 399 (1990).
 - ¹¹ Y. Kudoh, M. Tokonami, S. Miyazaki, and K. Otsuka, *Acta Metall. Mater.* **33**, 2049 (1985).
 - ¹² A. E. Dwight, R. A. Conner, Jr., and J.W. Downey, *Acta Crystallogr.* **18**, 835 (1965).
 - ¹³ V.E. Gunter, *Shape-Memory Effects and its Application in Medicine* (Nauka, Novosibirsk, 1992).
 - ¹⁴ J. Cai *et al.*, *Phys. Rev. B* **60**, 15 691 (1999).

- ¹⁵ E. V. Savushkin, V. B. Lapin, and V. E. Egorushkin. *J. Phys.: Condens. Matter.* **3**, 9185 (1991).
- ¹⁶ W. C. Mackrodt, E. A. Simpson, and N. M. Harrison, *Surf. Sci.* **384**, 192 (1997).
- ¹⁷ D. Vogtenhuber, *et al.*, *Phys. Rev. B* **49**, 2099 (1994).
- ¹⁸ M. Ramamoorthy, D. Vanderbilt, and R. D. King-Smith. *Phys. Rev. B* **49**, 16 721 (1994).

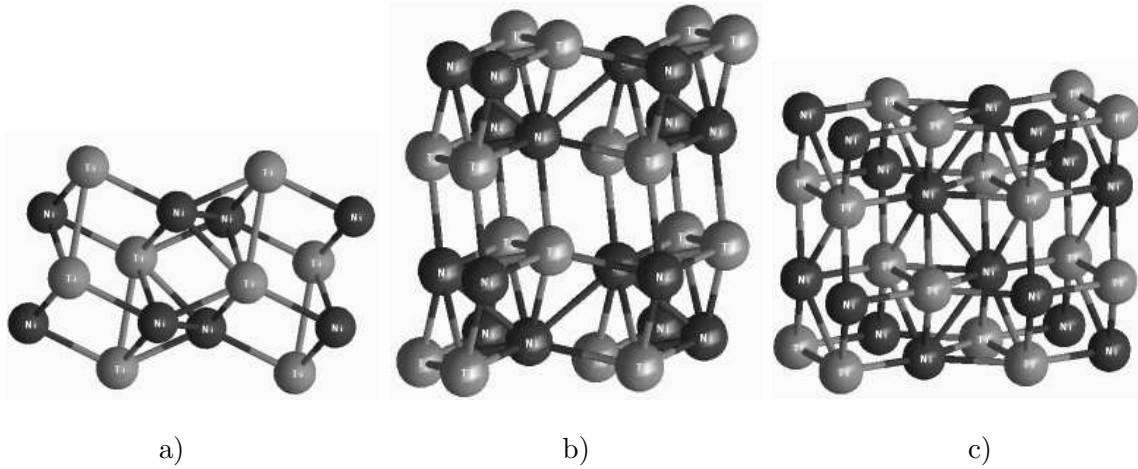
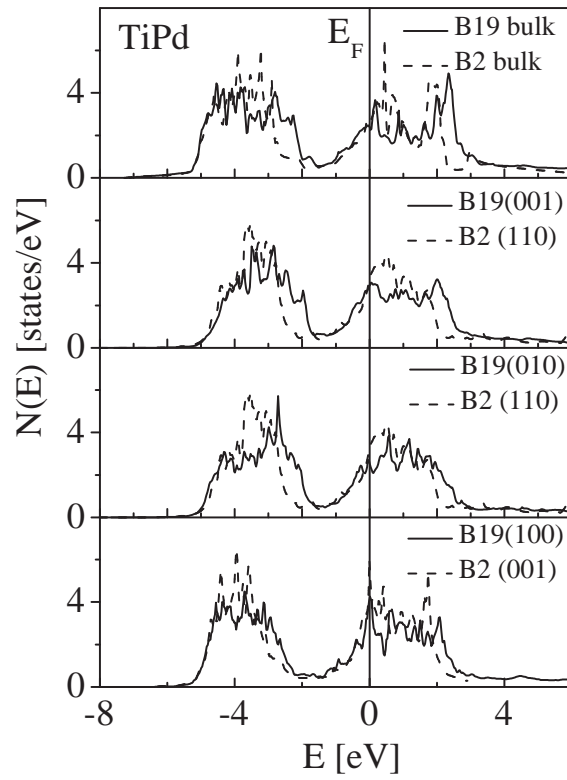
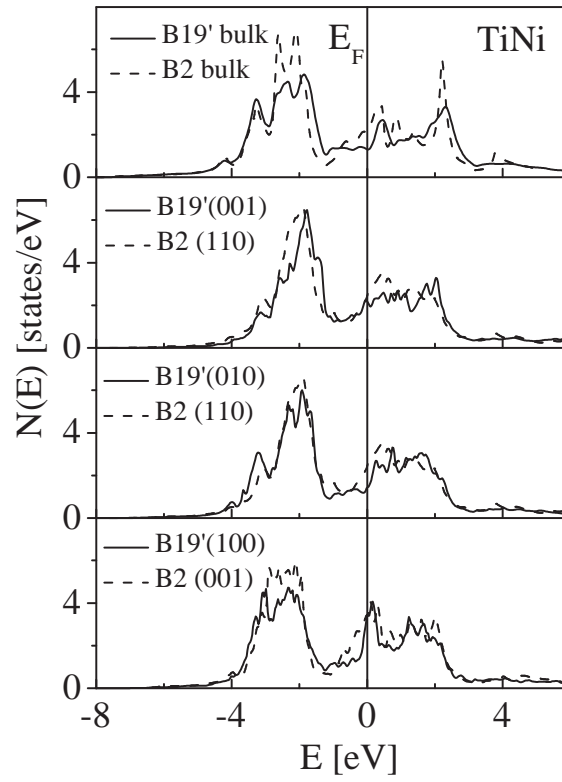


FIG. 1: Atomic structure of the $B19'$ -TiNi (100), (010) and (001) surfaces, respectively (side view). Upper part of slabs used for calculations is given only.



a)

b)

FIG. 2: The surface ES of $B19'$ -TiNi and $B19$ -TiPd (solid lines) in comparison with corresponding ones for parent $B2$ -phase (dashed lines).

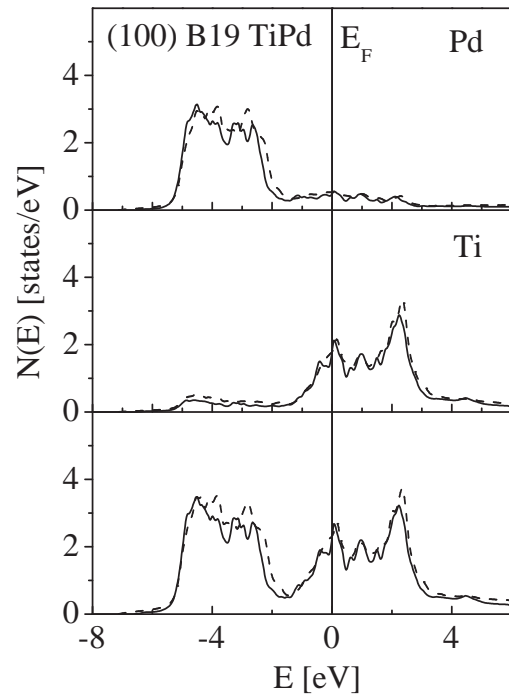
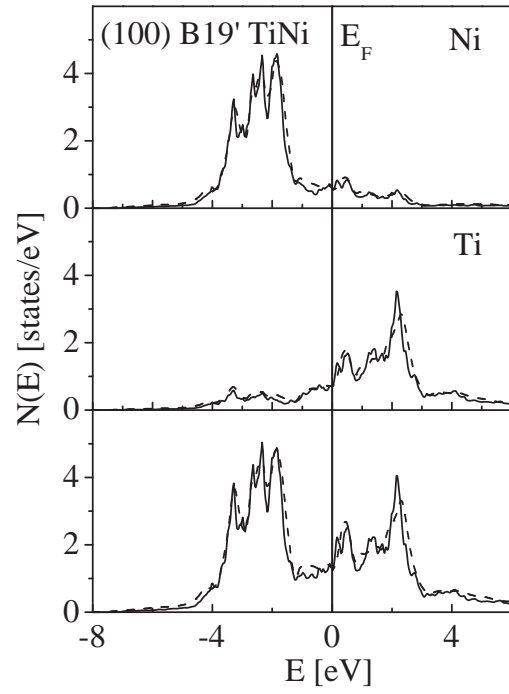
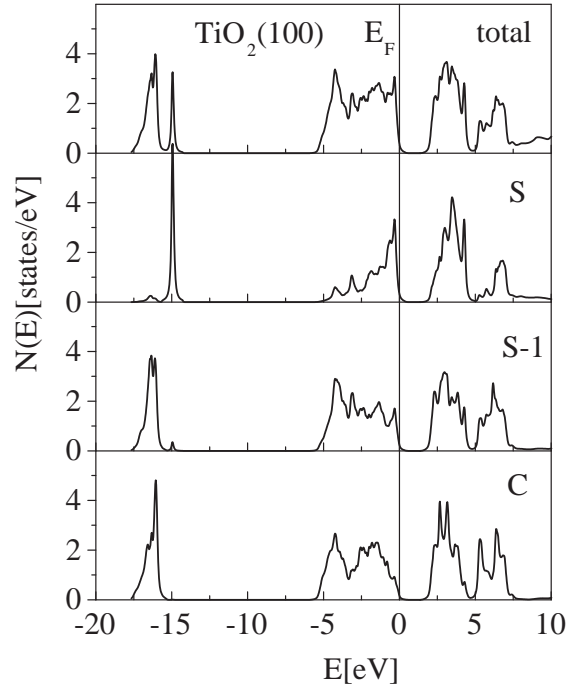
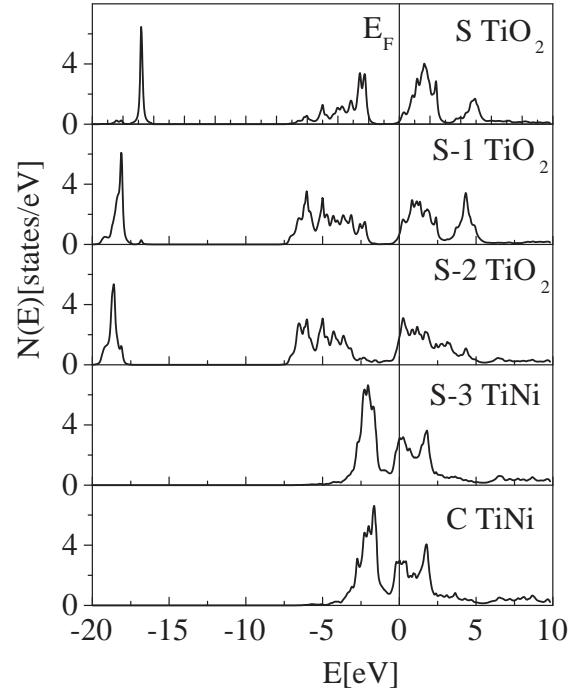


FIG. 3: The calculated LDOS of central layers and their sum for $B19'$ -TiNi (100) surface (solid lines) in comparison with DOS for bulk alloy (dashed lines).



a)

b)

FIG. 4: The layer-resolved DOS for TiO_2/TiNi system in comparison with results for clean TiO_2 (100) surface. The symbols S and C mark the surface and central layers, S-1, S-2, S-3 correspond to the position from the surface.